applied sciences

MDPI

Article

Numerical Modelling of Erythrocyte Sticking Mechanics

Raimondas Jasevičius

Institute of Mechanical Science, Faculty of Mechanics, Vilnius Gediminas Technical University, J. Basanavičiaus g. 28, LT-03224 Vilnius, Lithuania; raimondas.jasevicius@vilniustech.lt

Abstract: The mechanics of thrombus formation includes the interaction of platelets, fibrin, and erythrocytes. The interaction was analyzed as the erythrocyte approaches the activated platelet and fibrin thrombus formation. The discrete element method (DEM) was used for the numerical experiment. Details of numerical experiments are presented by analyzing the dynamics of an erythrocyte in the process of interaction; a history of force, velocity, and displacement is given. It is usually assumed that the objects modeled by the DEM can oscillate during the sticking process. Modeling only this requires specialized knowledge and long-term research. However, by taking into account the influence of the fluid and modeling a soft biological cell, a completely different behavior can be achieved using the DEM method. The results of the numerical experiment show the different behavior of the erythrocyte when it interacts with a certain surface. Without taking into account the influence of the fluid in the sticking process, oscillations of the erythrocyte are observed. Meanwhile, after evaluating the influence of the liquid on the sticking process, there are no oscillations and unloading processes, which are typical for ultrafine objects. It is hoped that this will contribute to the study of the complex process of thrombus formation.

Keywords: simulation; DEM; blood vessel; erythrocyte; clot

check for updates

Citation: Jasevičius, R. Numerical Modelling of Erythrocyte Sticking Mechanics. *Appl. Sci.* **2022**, *12*, 12576. https://doi.org/10.3390/app122412576

Academic Editors: Antonio Boccaccio, Dario Di Stasio, Maria Contaldo, Andrea Ballini and Michele Covelli

Received: 26 October 2022
Accepted: 5 December 2022
Published: 8 December 2022

Publisher's Note: MDPI stays neutral with regard to jurisdictional claims in published maps and institutional affiliations.

Copyright: © 2022 by the author. Licensee MDPI, Basel, Switzerland. This article is an open access article distributed under the terms and conditions of the Creative Commons Attribution (CC BY) license (https://creativecommons.org/licenses/by/4.0/).

1. Introduction

Erythrocytes (red blood cells, RBC) are one of the main components of the blood clot, which is still the focus of research to this day. The implications of the theory of erythrocyte motion in narrow capillaries is given by Fitz-Gerald [1]. An erythrocyte in the form of a drop of liquid is analyzed by Fischer et al. [2]. The dynamics of erythrocyte motion in filtration tests are given by Cokelet [3]. RBC rheology was analyzed by Shiga et al. [4] and Maeda [5]. The erythrocyte velocity was measured by Zhong et al. [6]. Erythrocyte dynamics in human retinal capillaries were investigated by Gu et al. [7].

One of the important problems associated with human health is the formation of a blood clot and blockage of a blood vessel. There are various cases and causes of blood clots. Risk factors for venous thrombosis have been reviewed by Rosendaal [8]. An association between atherosclerosis and venous thrombosis has been investigated by Prandoni et al. [9]. Stent thrombosis in the modern era was introduced by Cutlip et al. [10]. The formation of blood clots on biomaterial implants was analyzed by Shiu et al. [11]. Erythrocyte aggregation and its various structures were analyzed by Baskurt and Meiselman [12]. Farsaci et al. [13] analyzed whether the formation of a blood clot is a reversible process. Analysis of erythrocyte aggregation, taking into account rouleaux and clot formation, was given by Wagner et al. [14]. The contraction of the blood clot considering internal and external fibrinolysis was given by Tutwiler et al. [15].

There should always be solutions to deal with blood clot related problems. Shape memory alloys can be used to filter a blood clot (Tzou et al. [16]). Recently, cell-related research in the biological and medical sciences remains relevant, requiring new ideas, interdisciplinary research applications, and knowledge in the field of mechanics [17–26].

A boundary conditions investigation to improve computer simulation of cerebrospinal fluid dynamics in hydrocephalus patients is given in [27]. Their results suggested using

the computational fluid dynamic method and the fully coupled fluid-structure interaction method for cerebrospinal fluid dynamic analysis in patients with external and internal hydrocephalus, respectively. A new definition for intracranial compliance to evaluate adult hydrocephalus was suggested in [28]. The results of the present noninvasive study may be useful for future studies to link the clinical nonuniformities and variations of these patients with the nonuniform and oscillatory changes of the long-term intracranial compliance. Minimizing thermal damage to vascular nerves while drilling calcified plaque was investigated in [29]. Here, the load cell was attached to the tube wall to measure radial force.

In this work, the study is limited to the interaction of a single erythrocyte, while in further studies it would be possible to take into account the mechanical behavior under dynamics of a thrombus as an agglomerate. The presented model is universal, for example, it allows one to additionally study thrombus formation in the atria, as well as the further movement of a thrombus towards the brain and inside it [30].

2. Problem Formulation

Thrombosis is usually caused by damage to the wall of the blood vessel, blood composition, and increased blood clotting. In this work, a part of thrombus formation was chosen for study, i.e., when the erythrocyte begins to interact with fibrin and activated platelets. The problem is related to the interaction of the erythrocyte in the process of sticking. The purpose of this study is to achieve erythrocyte adhesion in a numerical experiment based on the initial data taken from known physical experiments. At the same time, using the developed theoretical model, the work is also aimed at reproducing the dynamics of erythrocytes, showing the behavior of erythrocyte interactions over time. According to previous studies [31], an erythrocyte is not prone to adherence, even when deformed at a distance from the vessel surface. However, during the formation of a clot, its behavior should involve the adhesion process, the behavior and mechanics of which are not clear. In this work, the main attention is paid to solving the above problem using the numerical simulation method. Additionally, the mechanical parameters of the thrombus components (platelets, fibrin) taken from the known literature are presented.

The question arises of how the behavior of cells can be different when sticking in a liquid. Mechanical parameters (Table 1) are taken from known physical experiments and used in the presented developed model. Taking into account these parameters, in this work, the interaction at a distance of a blood cell is reproduced and modeled. At the same time, different behavior of the cell during interaction was obtained, different modeling possibilities were shown, and attention was paid to the influence of the liquid. One of the objectives of the study is to obtain the sticking process, in which the erythrocyte (red blood cell) oscillates on the interacting surface. However, as further studies will show, oscillations under the action of a fluid (due to the drag force) may not occur. It is under the action of the liquid that the erythrocyte can be additionally deformed (only the process of loading occurs) when interacting with the surface, and because of which the erythrocyte stops as a result.

The first stage of the study of the interaction of red blood cells (RBC), presented in the publication [31], concerned the question of whether a blood cell can reach the surface of a blood vessel (the case when a thrombus is not formed); such a study of cell mechanics was not found in the known literature. The revealed effects were not previously observed, namely, the deformation of the cell in the absence of contact. This has become possible for soft matter such as a cell. In the second case, the present publication took the next step. In this case, the interaction of an erythrocyte cell with a blood clot was considered. This stands out as a separate case in clot formation when RBC adhere to the clot surface. Moreover, a completely different behavior of the cell was found than the accepted idea of the process of cell adhesion in air. The sticking process (with oscillations) in the liquid did not occur; this effect was not observed in the known literature. This is manifested in the completely different behavior of cells when interacting in liquid and when interacting in air.

The tasks are completely different, but since in both cases the object is the same—an erythrocyte, and the interaction takes place in a blood vessel, the descriptions of the simulation methodology have some similarities. The initial data are supplemented with data on the blood clot, and the additional forces required to solve the new problem are estimated. Part of the description of the methodology, i.e., a detailed description of the forces, is presented in [31] and is not repeated here.

3. Methodology

The discrete element method (DEM) makes it possible to virtually describe the motion of various objects from very small objects (e.g., atoms) to very large objects (e.g., planets). It is important that Newton's second law is applicable and suitable for describing the motion of these objects. Different objects have different mechanical properties, which are important to identify in advance from known physical experiments. Initially, the discrete element method was used to simulate the movement of large objects (rock masses, granular soils). In this paper, DEM is used for numerical simulation of cell interaction. Translational motion (of each i-th erythrocyte) is described by Newton's second law:

$$m_i \frac{d^2 \boldsymbol{x}_i}{dt^2} = \boldsymbol{F}_i(t) \tag{1}$$

where m_i and vector $\boldsymbol{x}_i$ are the mass and position of the i-th erythrocyte (red blood cell). The vector $\boldsymbol{F}_i(t) = \sum_j \boldsymbol{F}_{i,j}(t)$ corresponds to the resultant forces acting on the cell i in the event of possible interaction. Equation (1) is integrated with the 5th–order Gear predictor–corrector scheme [31].

During the interaction (Figure 1) of an erythrocyte, four main processes (approach, load, unload, separation) can be distinguished. Initially, the erythrocyte is close to the blood clot and interaction is possible. Figure 1 shows a model of the interaction of erythrocytes (red blood cells). The constitutive model of interaction can be described by the certain points (S-L-U-A′-E). When approaching (S-L), the movement of the erythrocyte corresponds to the interaction at a distance. At distances of load (L-U), unload (U-A′), reload-reunload (A′-E), the erythrocyte is in contact with the surface of the vessel. The force-displacement diagram is presented in Figure 1.

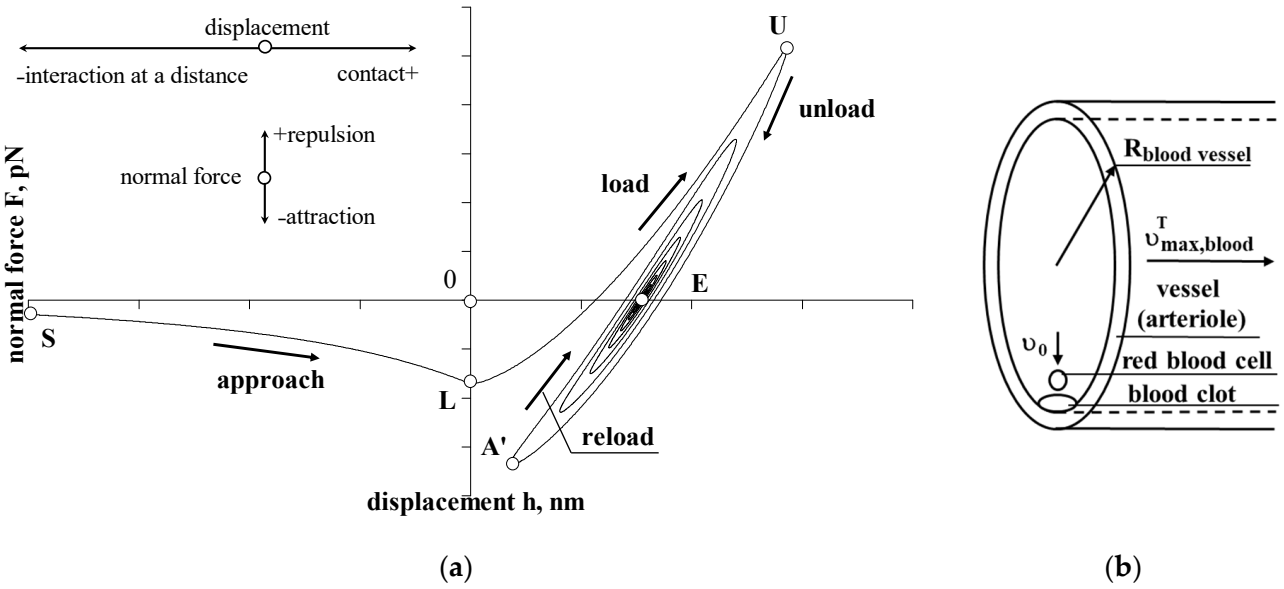

Figure 1. Sticking process model (**a**) and initial position of the erythrocyte (**b**). If it does not have enough kinetic energy to detach, reloading begins at point A′ and then the interaction ends at point E.

The additional effect of cell elongation (formation of a neck in the contact zone) during unloading was not taken into account in this work. Previously, this effect (additional elongation) was considered for softer structures such as virus spikes (Jasevičius [32]). In the future, it is planned to create an additional model (for erythrocyte interaction) that will allow us to evaluate the possible elongation of cells during unloading. It should be noted, as later shown by the results of the numerical experiment, that this effect is not achieved during unloading during adhesion/sticking (the cell does not reach the value h = 0 when unloading; therefore, for h < 0, no additional elongation will be observed). This effect may be important if it is necessary to separate an attached cell from a surface (e.g., the surface of a blood vessel). As mentioned earlier, the results show that the adhesion/sticking process may not reach this effect (additional elongation). However, this effect would be important in studying the detachment of the virus from the surface (rupture of spikes at separation virus from a cell surface) when additional elongation of the spike could be observed (Jasevičius [32]).

The interaction of the erythrocyte is described by the application of a total force:

$$F(t) = F_{el}(t) + F_{adh}(t) + F_{dl}(t) + F_{adh,diss}(t) + F_{viscous}(t) \quad (2)$$

where $F_{el}(t)$ is the elastic force, $F_{adh}(t)$ is the adhesion force, $F_{dl}(t)$ is the electrostatic double layer force, $F_{adh,diss}(t)$ is the adhesive-dissipative force and $F_{viscous}(t)$ is the viscous damping force. In this work, the problem is the dynamics of the cell; therefore, both force and displacement are not controlled in time; the resulting values (force, velocity, displacement) are obtained only after integrating non-linear force-displacement equations (integrated with the 5th Gear predictor–corrector scheme).

3.1. Approach, Interaction at a Distance

The expression for the total force acting on an erythrocyte at a distance can be represented:

$$F(t) = F_{adh}(t) + F_{dl}(t) + F_{drag}(t) \quad (3)$$

where $F_{adh}(t)$ is the adhesion force, $F_{dl}(t)$ is the electrostatic double layer force, and $F_{drag}(t)$ is the drag force. A description of each force (interaction at a distance) is presented by Jasevičius [31]. To describe the hydrodynamic force, the Stokes' drag force $F_{drag}(t) = 6 \cdot \pi \cdot \eta \cdot R_H \cdot v_{relative}(t)$ is used. In this equation, η is the viscosity of the fluid, $v_{relative}$ is the relative velocity in the normal direction, and R_H is the hydrodynamic radius of the red blood cell. For this simulation, it is assumed that $R_H = R_i$. The relative velocity is calculated considering $v_{relative}(t) = v_i(t) - v_{blood}(t)$. Here, v_i is the cell velocity in the normal direction and v_{blood} is the blood velocity in the normal direction.

3.2. Load, Contact

During the load and contact, the total force is:

$$F(t) = F_{L,adh} + F_{dl}(t) + F_{el}(t) + F_{drag}(t) \quad (4)$$

where $F_{L,adh}(t)$ is the adhesion force at point L (Figure 1), $F_{dl}(t)$ is the electrostatic double layer force, $F_{drag}(t)$ is the drag force, and $F_{el}(t)$ is the elastic force (Hertz model). A description of each force (load) is presented by Jasevičius [31]. During contact with the surface, the erythrocyte is deformed.

3.3. Unload, Contact

Unloading begins after reaching the maximum displacement of the erythrocyte under load. The general expression for the total force is:

$$F(t) = F_{el}(t) + F_{L,adh} + F_{adh,diss}(t) + F_{dl}(t) + F_{el}(t) + F_{drag}(t) + F_{viscous}(t) \quad (5)$$

where $F_{el}(t)$ is the elastic force (Hertz model), $F_{L,\ adh}(t)$ is the adhesion force at point L (Figure 1), $F_{adh,diss}(t)$ is the dissipative adhesion force, $F_{dl}(t)$ is the electrostatic double layer force, $F_{drag}(t)$ is the drag force, and $F_{viscous}(t)$ is the viscous damping force. A description of each force (unload) is presented by Jasevičius [31].

Energy dissipation due to adhesion. Energy dissipation $W_{adh,diss}$ due to the change in influence of adhesion can be described theoretically (Jasevičius [31]):

$$W_{adh,diss} = k_H \cdot \left| F_{L,adh} \cdot a_{F=0} \right| \tag{6}$$

where $F_{L,adh}$ is the adhesion force at point L (Figure 1), $a_{F=0}$ is the initial interaction distance at which the equilibrium of molecular attraction and repulsion potentials is assumed; it is considered as the minimum molecular center separation. The coefficient k_H gives ability to consider the different amount of energy dissipation. In this simulation, this coefficient is equal to $k_H = 1$. The dissipative adhesive force is described by the following equation:

$$F_{adh,diss}(t) = -\frac{2W_{adh,diss}}{h_U + a_{F=0}} \cdot \overline{h}(t) \tag{7}$$

where $\overline{h}(t)$ is the normal strain and $\overline{h}(t) = \frac{h_U - h(t)}{h_U}$ and depends on the maximum overlap (displacement) h_U.

Energy dissipation due to viscous damping. To simulate the dissipative behavior of an erythrocyte during the sticking process, a viscous damping model is taken into account. During dissipative oscillations, the kinetic energy of the erythrocyte is dissipated into heat. The viscous model is described based of the Tsuji model (Tsuji et al. [33], Jasevičius and Kruggel-Emden [34]):

$$F_{viscous}(t) = \alpha_d \sqrt{m_{eff} K_{el}(t)} \cdot \overline{h}(t) \cdot \left(-\dot{h}(t) \right) \tag{8}$$

where α_d is the damping coefficient and $\dot{h}(t)$ is the displacement rate (velocity) [34]. The stiffness $K_{el}(t)$ of the erythrocyte is taken into account (Hertz model) according to the equation:

$$K_{el}(t) = \frac{2}{3} E_{eff} \sqrt{R_{eff} h(t)} \tag{9}$$

where E_{eff} is the effective modulus of elasticity of the erythrocyte and blood clot, while R_{eff} represents the effective radius.

When an erythrocyte interacts with the boundary, the effective mass m_{eff} is equal to the mass $m_{eff} = m_i$ of the erythrocyte, since the boundary mass m_j (blood clot) is considered to be significantly greater than the mass of the erythrocyte $m_j \gg m_i$.

In the general case, the effective mass m_{eff} of interacting bodies is determined by the expression:

$$m_{eff} = \left(\frac{1}{m_i} + \frac{1}{m_j} \right)^{-1}. \tag{10}$$

The following process is the reload. This takes into account the decrease in the influence of viscous damping during unloading. The effect of attraction due to adhesion in contact is considered to be time dependent.

3.4. Reload and Reunload, Contact

Upon reaching the point of unloading A′, a reload of the erythrocyte may occur.

The equation for the total force is:

$$F(t) = F_{L,adh} + F_{adh,diss}(t) + F_{dl}(t) + F_{el}(t) + F_{drag}(t) + F_{viscous}(t) \tag{11}$$

where $F_{L,\ adh}(t)$ is the adhesion force at point L (Figure 1), $F_{dl}(t)$ is the electrostatic double layer force, $F_{drag}(t)$ is the drag force, and $F_{el}(t)$ is the elastic force (Hertz model). A descrip-

tion of each force is presented by Jasevičius [31]. $F_{adh,diss}(t)$ is the adhesive-dissipative force (Equation (7)) and $F_{viscous}(t)$ is the viscous damping force (Equation (8)).

If there were occasions when an erythrocyte would detach from the surface during unloading, this could be considered as a detachment (separation) process. When modeling the sticking process in this work, the separation process was not achieved and therefore was not analyzed further. A description of the process of separation of an erythrocyte can be found in Jasevičius [31].

4. Numerical Experiment

In a numerical experiment, it is planned to study the interaction of an erythrocyte with the surface of the blood clot. The aim is to analyze the effect of fluid on the process of erythrocyte sticking. As a result, the study of the sticking process is divided into two parts. In the first part, when the influence of the liquid is partially evaluated, the drag force is not taken into account and the electrostatic double layer force is taken into account. In the second part, all the forces presented in this article acting on the erythrocyte are evaluated. The initial experimental data are presented in Table 1.

Table 1. Initial data.

Objects	Initial Parameters	Values	References, Sources
Erythrocyte (red blood cell)	Diameter, d_i	6.2 µm	Turgeon [35]
	Initial interaction distance, $a_{F=0}$	20 nm	Jasevičius [31]
	Initial velocity, v_0	−0.010783 cm/s	Jasevičius [31]
	Mass, m_i	28 pg (picograms)	MediaLab, Inc. [36]
	Density, ρ_i	1.12 g/cm^3	Kumar et al. [37]
	Young's modulus, E_i	26 kPa	Dulińska et al. [38]
	Poisson's ratio, ν_i	0.5	Abay et al. [39]
	Surface potential, ψ_i	−24 mV	Pei et al. [40]
	Surface charge density ξ_i	−3 mC/m^2	Rubenstein et al. [41]
	The adhesion force at point A, $F_{A,adh,h=0}$ (between erythrocyte and fibrin)	−82.25 pN (79 ± 3 pN)	Carvalho et al. [42]
	The adhesion force at point L, $F_{L,adh,h=0}$ (erythrocyte–fibrin)	−38 pN	-
	Adhesive dissipative energy, $W_{adh,diss}$	$76 \cdot 10^{-20}$ J	-
Fibrin	Young's modulus, E_j	4 Mpa	Liu et al. [43]
	Density, ρ_i	1.33 g/cm^3	Zhmurov et al. [44]
Endothelial cell	Surface charge density ξ_j	−12 mC/m^2	Rubenstein [41]
Platelet (thrombocyte)	Density, $\rho_{platelet}$	1.067 g/cm^3	Thompson et al. [45]
	Young's modulus, $E_{platelet}$	10.0 kPa	Radmacher et al. [46]
	Poisson ratio, $\nu_{platelet}$	0.5	Radmacher et al. [46]
	Diameter, $d_{platelet}$ (non activated)	3.0 µm	Seyoum et al. [47]
Blood	PH	7.4	Wilschut [48]
	Temperature, T_{temp}	36.8 °C	Jasevičius [31]
	The permittivity of the free space, ε_0	$8.854 \cdot 10^{-12}$ C^{2}J^{-1}m^{-1}	Jasevičius [31]
	Debye length, λ	≈ 8.0 µm	Rubenstein [41]
	A dielectric constant of water, ε	74.5	Butt et al. [49]
	Blood flow velocity, $v^T_{max,blood}$	−3.0 cm/s	Nagaoka and Yoshida [50]
	Blood flow velocity at $a_{F=0} = 20$ nm distance in normal direction, v_S	−0.010783 cm/s	Jasevičius [31]
	Viscosity, η_f	3 cP(0.003 Pa·s)	Nacev et al. [51]

Table 1. *Cont.*

Objects	Initial Parameters	Values	References, Sources
Arteriole	Diameter, $d_{blood\ vessel}$ Surface potential, ψ_j	100 µm −48.3 mV	Nagaoka and Yoshida [50] Nakashima et al. [52]
Blood clot	Poisson ratio, ν_j	0.5	Tutwiler et al. [53]
Simulation	Time step	5 ps (picoseconds)	-

The results of the experiment in the first part are presented in Figure 2a–d. The graphs show the corresponding points of the interaction process path S-L-U-A′-E. The values of force, displacement, and velocity at these points are given in Table 2. In the first part of the study, contact of an erythrocyte is observed in the presence of interaction with a thrombus. This is due to the weakening of the electrostatic double layer force when the erythrocyte interacts with the forming blood clot. It is assumed that the sticking process begins when the erythrocyte reaches point A′, when the kinetic energy is not enough to detach from the interaction surface and the reloading process begins. Oscillations are observed when the movement of the erythrocyte in the sticking process oscillates to a complete stop at point E. Moreover, at this moment, the erythrocyte stops further deformation, and the force and velocity values acting in the normal direction are equal to zero.

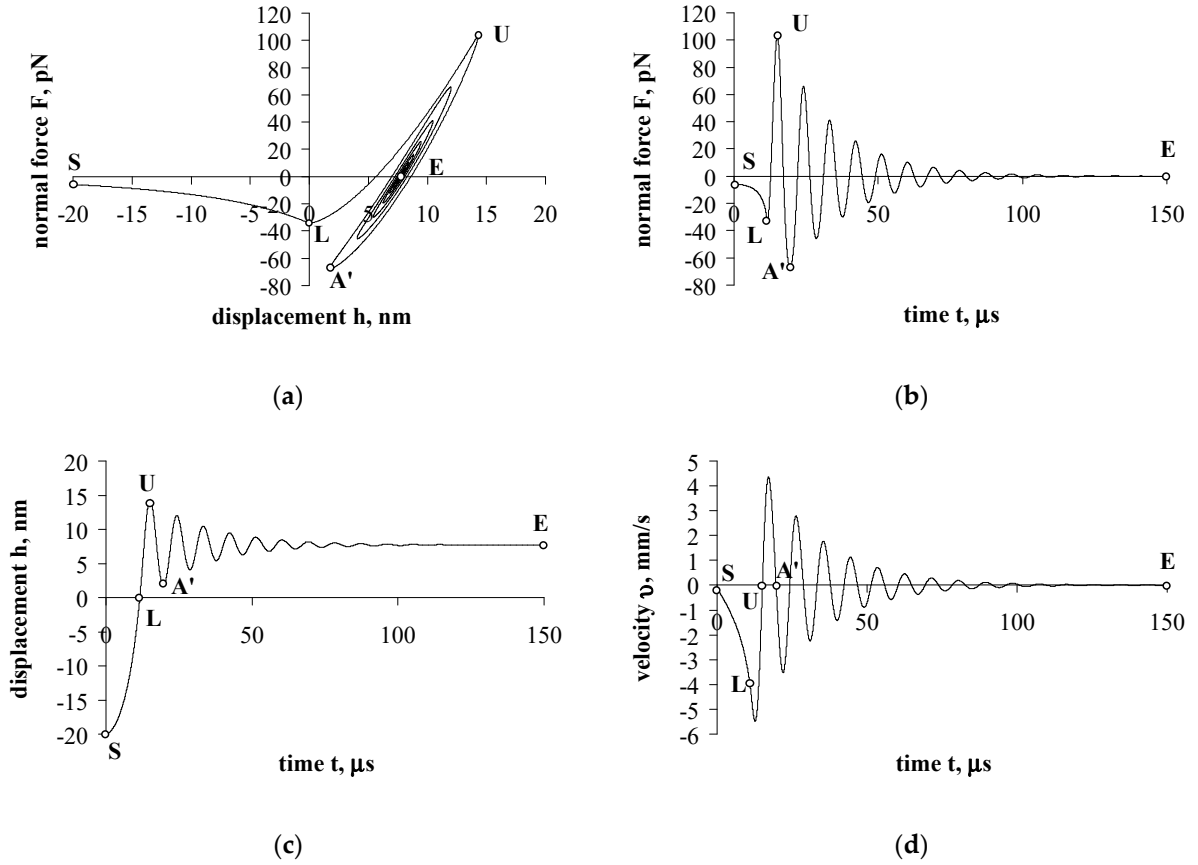

Figure 2. Interaction of an erythrocyte with a blood clot (fibrin and platelets). Without drag force. Dependence of the normal force on displacement (**a**) and time (**b**); dependence of displacement (**c**) and velocity (**d**) on time.

Table 2. Properties of the movement of an erythrocyte during interaction at certain points S-L-U-A′-E.

Parameter		Values at Certain Points				
		S	**L**	**U**	**A′**	**E**
Without drag force	t, μs	0	11.59687	15.120995	19.679315001	≈150
	F, pN	−5.78593	−34.27663	104.69451942	−66.7513884	0
	h, nm	−20	0	14.3479743	1.806173644	7.71084038
	v, mm/s	−0.10783	−4.6735475	0	0	0
With drag force	t, μs	0	107.64	≈250	-	≈250
	F, pN	−5.78593	−0.18155	0	-	0
	h, nm	−20	0	7.562478	-	7.562478
	v, mm/s	−0.10783	−0.30232	0	-	0

In the process of sticking, during oscillations, the values of the normal velocity change; positive and negative values are observed. Such obtaining results are likely if, for example, a dry particle or a drop of water interacts with a certain surface in the air. It should be noted that oscillations of an ultrafine object are difficult to physically detect, especially if the deformation occurs only in the contact zone (Jasevicius and Kruggel-Emden [34]).

The results of the second part of the experiment are presented in Figure 3a–d. The graphs show the corresponding points of the interaction process path S-L-U(E); the values of force, displacement, and velocity at these points are given in Table 2. In the case of such an interaction, the drag force is considered. The results obtained (Figure 3) are completely different from Figure 2. Not only do the achieved values of forces, displacements, and velocities differ, but so does the behavior of the erythrocyte itself. During oscillations, the sticking process is absent. The movement of an erythrocyte stops when it is deformed at the point E on the corresponding surface. The values of force and velocity (Figure 3) of the adhered cell, as in Figure 2, are equal to zero. Moreover, when comparing the results (Figures 2 and 3), it can be noted that until the erythrocyte movement stops under the action of the drag force (Figure 3), the interaction time lasts longer. In the case of sticking (Figure 3), the velocity value remained negative until it decreased and reached zero.

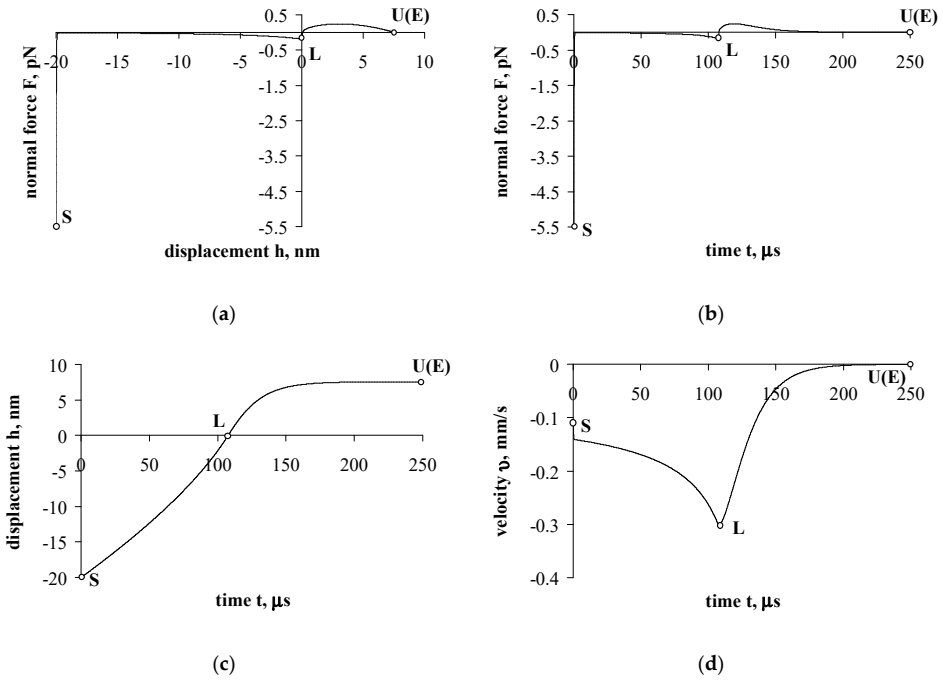

Figure 3. Interaction of an erythrocyte with a blood clot (fibrin and platelets) with drag force. Dependence of the normal force on displacement (**a**) and time (**b**); dependence of displacement (**c**) and velocity (**d**) on time.

During the sticking process, adhesion effects are quickly suppressed but sufficient for the erythrocyte to approach the surface and adhere. It was also observed that the unloading process did not occur; point U, which should describe the beginning of unloading, coincided with point E, indicating the end of the erythrocyte sticking process. If the interaction of an erythrocyte in air is modeled, then point U must coincide with the maximum force achieved. However, the influence of the liquid completely changed the behavior of the erythrocyte, and the load curve (force-displacement) itself, upon contact, has the form of an arc, and the value of the force at point U is zero. This would be unusual when simulating the interaction of an erythrocyte in air, but in a liquid such an interaction has become possible. Further research will focus on a more detailed study of the dynamics of thrombus components. The developed theoretical model can also be adapted to analyze the sticking process of other biological structures [32,54,55].

5. Conclusions

The paper analyzes the interaction of an erythrocyte with the surface of the corresponding clot. It was noticed that, without taking into account the drag force, oscillations occur during the interaction of the erythrocyte. When the influence of the fluid is evaluated and a drag force is applied, it completely changes the behavior of the erythrocyte. Under the action of the drag force, there is no typical sticking process with oscillations in the movement of the erythrocyte. Upon contact, the erythrocyte is deformed and, due to the action of adhesion forces, remains deformed and attached to the surface with a residual displacement.

This study is useful for studying the formation of a thrombus (blood clot), characterizing the dynamics of not only an individual erythrocyte, but also erythrocytes as a system. It can be noted that additional known mechanisms of thrombus formation, such as the formation of a fibrin network, will lead to a better process of aggregating the attached erythrocytes. Further research may be aimed at studying the mechanics of fibrin and activated platelets.

Funding: The research was funded by the Multidisciplinary Digital Publishing Institute (MDPI).

Institutional Review Board Statement: Not applicable.

Informed Consent Statement: Not applicable.

Data Availability Statement: Not applicable.

Conflicts of Interest: The authors declare no conflict of interest.

References

1. Fitz-Gerald, J.M. Implications of a theory of erythrocyte motion in narrow capillaries. *J. Appl. Physiol.* **1969**, *27*, 912–918. [CrossRef]
2. Fischer, T.M.; Stöhr-Lissen, M.; Schmid-Schönbein, H. The red cell as a fluid droplet: Tank tread-like motion of the human erythrocyte membrane in shear flow. *Science* **1978**, *202*, 894–896. [CrossRef]
3. Cokelet, G.R. Dynamics of erythrocyte motion in filtration tests and in vivo flow. *Scand. J. Clin. Lab. Investig.* **1981**, *41*, 77–82. [CrossRef]
4. Shiga, T.; Maeda, N.; Kon, K. Erythrocyte rheology. *Crit. Rev. Oncol. Hematol.* **1990**, *10*, 9–48. [CrossRef]
5. Maeda, N. Erythrocyte rheology in microcirculation. *Jpn. J. Physiol.* **1996**, *46*, 1–14. [CrossRef]
6. Zhong, Z.; Petrig, B.L.; Qi, X.; Burns, S.A. In vivo measurement of erythrocyte velocity and retinal blood flow using adaptive optics scanning laser ophthalmoscopy. *Opt. Express* **2008**, *16*, 12746–12756. [CrossRef]
7. Gu, B.; Wang, X.; Twa, M.D.; Tam, J.; Girkin, C.A.; Zhang, Y. Noninvasive in vivo characterization of erythrocyte motion in human retinal capillaries using high-speed adaptive optics near-confocal imaging. *Biomed. Opt. Express* **2018**, *9*, 3653–3677. [CrossRef]
8. Rosendaal, F.R. Venous thrombosis: A multicausal disease. *Lancet* **1999**, *353*, 1167–1173. [CrossRef]
9. Prandoni, P.; Bilora, F.; Marchiori, A.; Bernardi, E.; Petrobelli, F.; Lensing, A.W.; Prins, M.H.; Girolami, A. An association between atherosclerosis and venous thrombosis. *N. Engl. J. Med.* **2003**, *348*, 1435–1441. [CrossRef]
10. Cutlip, D.E.; Baim, D.S.; Ho, K.K.L.; Popma, J.J.; Lansky, A.J.; Cohen, D.J.; Carrozza, J.P.; Chauhan, M.S.; Rodriguez, O.; Kuntz, R.E. Stent thrombosis in the modern era: A pooled analysis of multicenter coronary stent clinical trials. *Circulation* **2001**, *103*, 1967–1971. [CrossRef]

11. Shiu, H.T.; Goss, B.; Lutton, C.; Crawford, R.; Xiao, Y. Formation of blood clot on biomaterial implants influences bone healing. *Tissue Eng. Part B Rev.* **2014**, *20*, 697–712. [CrossRef]
12. Baskurt, O.K.; Meiselman, H.J. Erythrocyte aggregation: Basic aspects and clinical importance. *Clin. Hemorheol. Microcirc.* **2013**, *53*, 23–37. [CrossRef]
13. Farsaci, F.; Tellone, E.; Galtieri, A.; Ficarra, S. Is a dangerous blood clot formation a reversible process? Introduction of new characteristic parameter for thermodynamic clot blood characterization: Possible molecular mechanisms and pathophysiologic applications. *J. Mol. Liq.* **2018**, *262*, 345–353. [CrossRef]
14. Wagner, C.; Steffen, P.; Svetina, S. Aggregation of red blood cells: From rouleaux to clot formation. *Comptes Rendus Phys.* **2013**, *14*, 459–469. [CrossRef]
15. Tutwiler, V.; Peshkova, A.D.; Le Minh, G.; Zaitsev, S.; Litvinov, R.I.; Cines, D.B.; Weisel, J.W. Blood clot contraction differentially influences internal and external fibrinolysis. *J. Thromb. Haemost.* **2019**, *17*, 361–370. [CrossRef]
16. Tzou, H.S.; Lee, H.-J.; Arnold, S.M. Smart materials, precision sensors/actuators, smart structures, and structronic systems. *Mech. Adv. Mater. Struct.* **2004**, *11*, 367–393. [CrossRef]
17. Zhou, E.H.; Lim, C.T.; Quek, S.T. Finite element simulation of the micropipette aspiration of a living cell undergoing large viscoelastic deformation. *Mech. Adv. Mater. Struct.* **2005**, *12*, 501–512. [CrossRef]
18. Marion, N.W.; Liang, W.; Liang, W.; Reilly, G.C.; Day, D.E.; Rahaman, M.N.; Mao, J.J. Borate glass supports the in vitro osteogenic differentiation of human mesenchymal stem cells. *Mech. Adv. Mater. Struct.* **2005**, *12*, 239–246. [CrossRef]
19. Lin, S.T.; Bhattacharyya, D.; Fakirov, S.; Matthews, B.; Cornish, J. A novel microfibrillar composite approach towards manufacturing nanoporous tissue scaffolds. *Mech. Adv. Mater. Struct.* **2014**, *21*, 237–243. [CrossRef]
20. Stano, P.; de Souza, T.P.; Carrara, P.; Altamura, E.; D'Aguanno, E.; Caputo, M.; Luisi, P.L.; Mavelli, F. Recent Biophysical Issues about the Preparation of Solute-Filled Lipid Vesicles. *Mech. Adv. Mater. Struct.* **2015**, *22*, 748–759. [CrossRef]
21. Chanda, A.; Callaway, C.; Clifton, C.; Unnikrishnan, V. Biofidelic human brain tissue surrogates. *Mech. Adv. Mater. Struct.* **2018**, *25*, 1335–1341. [CrossRef]
22. Abpeikar, Z.; Milan, P.B.; Moradi, L.; Anjomshoa, M.; Asadpour, S. Influence of pore sizes in 3D-scaffolds on mechanical properties of scaffolds and survival, distribution, and proliferation of human chondrocytes. *Mech. Adv. Mater. Struct.* **2021**, *29*, 4911–4922. [CrossRef]
23. Korayem, M.H.; Rastegar, Z. Development of 3D manipulation of viscoelastic biological cells by AFM based on contact models and oscillatory drag. *Mech. Adv. Mater. Struct.* **2021**, *28*, 2572–2584. [CrossRef]
24. Martynenko, A.; Zozulya, V.V. Mathematical modeling of the cardiac tissue. *Mech. Adv. Mater. Struct.* **2021**, *29*, 4506–4522. [CrossRef]
25. Asadi, A.; Hedayat, D.; Ghofrani, S.; Mehrizi, A.A.; Shadalooyi, G.; Kadkhodapour, J.; Anaraki, A.P. Modification of hexachiral unit cell to enhance auxetic stent performance. *Mech. Adv. Mater. Struct.* **2022**, 1–5. [CrossRef]
26. Li, N.; Zhuo, Q.; Yu, K.; Dong, W.; Chen, D.; Zheng, R. Bionic bone structure: Establishment of joint model based on bone nanopores structure and its mechanical behavior and biocompatibility. *Mech. Adv. Mater. Struct.* **2022**, *29*, 1072–1079. [CrossRef]
27. Gholampour, S.; Fatouraee, N. Boundary conditions investigation to improve computer simulation of cerebrospinal fluid dynamics in hydrocephalus patients. *Commun. Biol.* **2021**, *4*, 394. [CrossRef] [PubMed]
28. Gholampour, S.; Yamini, B.; Droessler, J.; Frim, D. A New Definition for Intracranial Compliance to Evaluate Adult Hydrocephalus After Shunting. *Front. Bioeng. Biotechnol.* **2022**, *10*, 900644. [CrossRef] [PubMed]
29. Gholampour, S.; Hajirayat, K. Minimizing thermal damage to vascular nerves while drilling of calcified plaque. *BMC Res. Notes* **2019**, *12*, 338. [CrossRef]
30. Gholampour, S.; Balasundaram, H.; Thiyagarajan, P.; Droessler, J.; Yamini, B. A mathematical framework for the dynamic interaction of pulsatile blood, brain, and cerebrospinal fluid. *Comput. Methods Programs Biomed.* **2022**, 107209. [CrossRef]
31. Jasevičius, R. Numerical modeling of red blood cell interaction mechanics. *Mech. Adv. Mater. Struct.* **2022**, 1–8. [CrossRef]
32. Jasevičius, R. Numerical modeling of coronavirus interaction mechanics with a host human cell. *Mech. Adv. Mater. Struct.* **2022**, *29*, 2186–2196. [CrossRef]
33. Tsuji, Y.; Tanaka, T.; Ishida, T. Lagrangian numerical simulation of plug flow of cohesionless particles in a horizontal pipe. *Powder Technol.* **1992**, *71*, 239–250. [CrossRef]
34. Jasevičius, R.; Kruggel-Emden, H. Numerical modelling of the sticking process of a S. aureus bacterium. *Int. J. Adhes. Adhesiv.* **2017**, *77*, 15–28. [CrossRef]
35. Turgeon, M.L. *Clinical Hematology: Theory and Procedures*, 4th ed.; Lippincott Williams & Wilkins: Philadelphia, PA, USA, 2005; p. 570.
36. MediaLab, Inc. Checked Online 2022-04-04. Available online: https://www.labce.com/spg469924_initial_evaluation_of_rbc_morphology_from_automate.aspx (accessed on 4 December 2022).
37. Kumar, A.A.; Patton, M.R.; Hennek, J.W.; Lee, S.Y.R.; D'Alesio-Spina, G.; Yang, X.; Kanter, J.; Shevkoplyas, S.S.; Brugnara, C.; Whitesides, G.M. Density-based separation in multiphase systems provides a simple method to identify sickle cell disease. *Proc. Natl. Acad. Sci. USA* **2014**, *111*, 14864–14869. [CrossRef] [PubMed]
38. Dulińska, I.; Targosz, M.; Strojny, W.; Lekka, M.; Czuba, P.; Balwierz, W.; Szymoński, M. Stiffness of normal and pathological erythrocytes studied by means of atomic force microscopy. *J. Biochem. Biophys. Methods* **2006**, *66*, 1–11. [CrossRef] [PubMed]

39. Abay, A.; Simionato, G.; Chachanidze, R.; Bogdanova, A.; Hertz, L.; Bianchi, P.; Akker, E.V.D.; Von Lindern, M.; Leonetti, M.; Minetti, G.; et al. Glutaraldehyde—A subtle tool in the investigation of healthy and pathologic red blood cells. *Front. Physiol.* **2019**, *10*, 1–14. [CrossRef]
40. Pei, Q.; Hu, X.; Zheng, X.; Liu, S.; Li, Y.; Jing, X.; Xie, Z. Light-activatable red blood cell membrane-camouflaged dimeric prodrug nanoparticles for synergistic photodynamic/chemotherapy. *ACS Nano* **2018**, *12*, 1630–1641. [CrossRef]
41. Rubenstein, D.A.; Yin, W.; Frame, M.D. *Biofluid Mechanics: An Introduction to Fluid Mechanics, Macrocirculation, and Microcirculation*, 2nd ed.; Academic Press: London, UK, 2016; p. 544. [CrossRef]
42. Carvalho, F.A.; Connell, S.; Miltenberger-Miltenyi, G.; Pereira, S.V.; Tavares, A.; Ariëns, R.A.S.; Santos, N.C. Atomic force microscopy-based molecular recognition of a fibrinogen receptor on human erythrocytes. *ACS Nano* **2010**, *4*, 4609–4620. [CrossRef]
43. Liu, W.; Carlisle, C.R.; Sparks, E.A.; Guthold, M. The mechanical properties of single fibrin fibers. *J. Thromb. Haemost.* **2010**, *8*, 1030–1036. [CrossRef]
44. Zhmurov, A.; Protopopova, A.D.; Litvinov, R.I.; Zhukov, P.; Weisel, J.W.; Barsegov, V. Atomic structural models of fibrin oligomers. *Structure* **2018**, *26*, 857–868. [CrossRef] [PubMed]
45. Thompson, C.B.; Eaton, K.A.; Princiotta, S.M.; Rushin, C.A.; Valeri, C.R. Size dependent platelet subpopulations: Relationship of platelet volume to ultrastructure, enzymatic activity, and function. *Br. J. Haematol.* **1982**, *50*, 509–519. [CrossRef] [PubMed]
46. Radmacher, M.; Fritz, M.; Kacher, C.M.; Cleveland, J.; Hansma, P. Measuring the viscoelastic properties of human platelets with the atomic force microscope. *Biophys. J.* **1996**, *70*, 556–567. [CrossRef] [PubMed]
47. Seyoum, M.; Enawgaw, B.; Melku, M. Human blood platelets and viruses: Defense mechanism and role in the removal of viral pathogens. *Thromb. J.* **2018**, *16*, 1–6. [CrossRef] [PubMed]
48. Wilschut, J. *Membrane Fusion*; CRC Press: Boca Raton, FL, USA, 1990; p. 938. [CrossRef]
49. Butt, H.-J.; Graf, K.; Kappl, M. *Physics and Chemistry of Interfaces*; Wiley-VCH: Berlin, Germany, 2003; p. 495. [CrossRef]
50. Nagaoka, T.; Yoshida, A. Noninvasive evaluation of wall shear stress on retinal microcirculation in humans. *Investig. Ophthalmol. Vis. Sci.* **2006**, *47*, 1113–1119. [CrossRef]
51. Nacev, A.; Beni, C.; Bruno, O.; Shapiro, B. The behaviors of ferro-magnetic nano-particles in and around blood vessels under applied magnetic fields. *J. Magn. Magn. Mater.* **2011**, *323*, 651–668. [CrossRef]
52. Nakashima, M.; Mombouli, J.V.; Taylor, A.A.; Vanhoutte, P.M. Endothelium-dependent hyperpolarization caused by bradykinin in human coronary arteries. *J. Clin. Investig.* **1993**, *92*, 2867–2871. [CrossRef]
53. Tutwiler, V.; Litvinov, R.I.; Protopopova, A.; Nagaswami, C.; Villa, C.; Woods, E.; Abdulmalik, O.; Siegel, D.L.; Russell, J.E.; Muzykantov, V.R.; et al. Pathologically stiff erythrocytes impede contraction of blood clots. *J. Thromb. Haemost.* **2021**, *19*, 1990–2001. [CrossRef]
54. Jasevičius, R. Numerical simulation of the mechanics of oblique interaction of a bacterium with a flat surface. *Mech. Adv. Mater. Struct.* **2022**, *29*, 2884–2894. [CrossRef]
55. Jasevičius, R. Numerical modeling of the mechanics of the interaction of coronavirus with the lung epithelial cell. *Mech. Adv. Mater. Struct.* **2022**, *29*, 3030–3039. [CrossRef]